

## Data processing for the Active Particle-induced X-ray Spectrometer and initial scientific results from Chang'e-3 mission \*

Xiao-Hui Fu<sup>1</sup>, Chun-Lai Li<sup>1</sup>, Guang-Liang Zhang<sup>1</sup>, Yong-Liao Zou<sup>1</sup>, Jian-Jun Liu<sup>1</sup>, Xin Ren<sup>1</sup>, Xu Tan<sup>1</sup>, Xiao-Xia Zhang<sup>1</sup>, Wei Zuo<sup>1</sup>, Wei-Bin Wen<sup>1</sup>, Wen-Xi Peng<sup>2</sup>, Xing-Zhu Cui<sup>2</sup>, Cheng-Mo Zhang<sup>2</sup>, Huan-Yu Wang<sup>2</sup>

<sup>1</sup> National Astronomical Observatories, Chinese Academy of Sciences, Beijing 100012, China; [licl@nao.cas.cn](mailto:licl@nao.cas.cn)

<sup>2</sup> Institute of High Energy Physics, Chinese Academy of Sciences, Beijing 100049, China

Received 2014 July 21; accepted 2014 September 29

**Abstract** The Active Particle-induced X-ray Spectrometer (APXS) is an important payload mounted on the Yutu rover, which is part of the Chang'e-3 mission. The scientific objective of APXS is to perform in-situ analysis of the chemical composition of lunar soil and rock samples. The radioactive sources, <sup>55</sup>Fe and <sup>109</sup>Cd, decay and produce  $\alpha$ -particles and X-rays. When X-rays and  $\alpha$ -particles interact with atoms in the surface material, they knock electrons out of their orbits, which release energy by emitting X-rays that can be measured by a silicon drift detector (SDD). The elements and their concentrations can be determined by analyzing their peak energies and intensities. APXS has analyzed both the calibration target and lunar soil once during the first lunar day and again during the second lunar day. The total detection time lasted about 266 min and more than 2000 frames of data records have been acquired. APXS has three operating modes: calibration mode, distance sensing mode and detection mode. In detection mode, work distance can be calculated from the X-ray counting rate collected by SDD. Correction for the effect of temperature has been performed to convert the channel number for each spectrum to X-ray energy. Dead time correction is used to eliminate the systematic error in quantifying the activity of an X-ray pulse in a sample and derive the real count rate. We report APXS data and initial results during the first and second lunar days for the Yutu rover. In this study, we analyze the data from the calibration target and lunar soil on the first lunar day. Seven major elements, including Mg, Al, Si, K, Ca, Ti and Fe, have been identified. Comparing the peak areas and ratios of calibration basalt and lunar soil the landing site was found to be depleted in K, and have lower Mg and Al but higher Ca, Ti, and Fe. In the future, we will obtain the elemental concentrations of lunar soil at the Chang'e-3 landing site using APXS data.

**Key words:** data analysis — composition — Moon

---

\* Supported by the National Natural Science Foundation of China.

## 1 INTRODUCTION

The Active Particle-induced X-ray Spectrometer (APXS) permits the determination of elemental chemical composition of rocks and soil by placing its sensor head against the sample, powering on the instrument and acquiring spectra. It does not require any preparation of the sample and is thus well suited for in-situ measurements of the surface constituents of objects in space (e.g. planets, comets and asteroids). Characterizing rocks and regolith is critical for the geologic exploration of a planet's surface by rovers. Chemical analysis of the samples will be supported by mineralogical analysis and images of their texture, thus facilitating their classification (igneous, metamorphic, sedimentary, water depositional, etc.).

Three generations at Mars rovers all carried an APXS instrument as part of their science payload which used  $^{244}\text{Cm}$  as the radioactive source. The APXS that was carried by the Mars Pathfinder mission had three instrumental modes. The  $\alpha$ -mode measured the energy and intensity of backscattered  $\alpha$ -particles from a sample, which is also called Rutherford backscattering (RBS). The proton-mode measured the intensity of protons emitted from ( $\alpha$ , p) reactions in the sample, which enabled measurement of Na, Mg, Al, Si, S and N. The X-ray mode measured the intensities of X-rays produced from  $\alpha$ -particles and X-rays striking the sample, thus facilitating measurement of abundances of elements, which uses processes called  $\alpha$  particle induced X-ray emission (PIXE) and X-ray fluorescence (XRF) respectively. Unlike the Pathfinder APXS, the APXS that is part of the ongoing Mars Exploration Rover (MER) does not have a proton mode. The proton mode has been dropped because recent increases in spectral resolution and sensitivity in the X-ray mode have made it unnecessary. The APXS that is part of the Mars Science Laboratory (MSL) is an improved version of the APXS that flew successfully on Pathfinder and MER (Rieder et al. 1997, 2003; Gellert et al. 2006). The MSL APXS takes advantage of a combination of the well-established terrestrial standard methods PIXE and XRF to determine elemental chemistry. It uses sources of  $^{244}\text{Cm}$  for X-ray spectroscopy to determine the abundance of major elements down to trace elements from sodium to bromine and beyond.

Table 1 gives the APXS instruments in planetary missions and their radioactive sources, working principles and detection abilities.

The fundamental parameter approach has been widely used to derive the elemental composition from X-ray data and similarly least squares fitting programs have been used to reduce the alpha and proton data (Gellert et al. 2006). A new approach using fundamental parameters to derive constituent chemicals from APXS spectra has been developed by Campbell et al. (2009, 2010). It employs a spectral fitting code, GUAPX, which was developed from the PIXE analysis software package GUPIX (Maxwell et al. 1995) by adding the capability to handle simultaneous XRF analysis. GUAPX could fit the spectra, compute matrix effects and convert the peak areas to elemental concentrations. It has been used in data analysis of APXS instruments onboard MSL.

## 2 SCIENTIFIC OBJECTIVES

The scientific objectives of the Chang'e-3 mission include surveying lunar surface topography and geology, collecting data about material composition and resources on the lunar surface, measuring the Sun-Earth-Moon space environment and performing lunar-based astronomical observation (Ip et al. 2014). APXS is one of four scientific instruments aboard on the Yutu rover, which has the goal of performing in-situ analysis of the chemical compositions of lunar soils and rocks at the landing site.

APXS is a reliable, well-tested instrument for quantitative in-situ elemental analysis of planetary surfaces and has been successfully employed for surface exploration on Mars. APXS on Spirit and Opportunity together have analyzed hundreds of rocks and soils. The data they acquired significantly changed the view of Mars. Compositions of rock samples measured by APXS from Gusev Crater indicate they are mostly basalts, and are distinct from Martian meteorites. Prior to the MER missions, there was considerable controversy about whether great swaths of the Martian surface were covered

**Table 1** Comparisons of APXS Instruments in Lunar and Planetary Missions

Mission	Radioactive source	Working principle	Detector	Energy resolution	Detection ability	Reference
Mars Pathfinder	$9 \times {}^{244}\text{Cm}$ total 40mCi	RBS proton mode PIXE XRF	Si PiN	250 eV@5.9 keV	Determine all elements (except H) present in amounts above a fraction of a percent	Economou (2001); Foley et al. (2003)
MER	$6 \times {}^{244}\text{Cm}$ total 30mCi	RBS PIXE XRF	SDD 10 mm <sup>2</sup>	160 eV@5.9 keV	Determine light elements (C and O), major elements, such as Mg, Al, Si, K, Ca, and Fe, and several minor elements	Rieder et al. (2003); Gellert et al. (2006)
MSL	$6 \times {}^{244}\text{Cm}$	PIXE XRF	SDD 10 mm <sup>2</sup>	200 eV@6.4 keV	Determine the abundance of major elements down to trace elements from sodium to bromine and beyond	Campbell et al. (2012); Gellert et al. (2009)
Rosetta mission	$6 \times {}^{244}\text{Cm}$ total 30mCi	RBS PIXE XRF	SDD	180 eV@5.9 keV	Determine light elements (C and O), detect the elements from Na up to Ni and above	Schmanke et al. (2010); Klingelhöfer et al. (2007)
Beagle-2	$2 \times {}^{55}\text{Fe} +$ $2 \times {}^{109}\text{Cd}$	PIXE	Si PiN	300 eV	Determine major elements (Mg, Al, Si, S, Ca, Ti, Cr, Mn, Fe) and trace elements up to Nb	Pullan et al. (2004)
Chandrayaan-2	$6 \times {}^{244}\text{Cm}$	PIXE XRF	SDD 20 mm <sup>2</sup>	150 eV@5.9 keV	Determine elements from Na to Br	Shanmugam et al. (2014)
Chang'e-3	$4 \times {}^{55}\text{Fe} +$ $4 \times {}^{109}\text{Cd}$	PIXE XRF	SDD 7 mm <sup>2</sup>	135 eV@5.9 keV	Determine major element concentration $\geq 0.1\text{wt}\%$	This study

with andesite. The Opportunity rover encountered sedimentary rocks which APXS indicated have high contents of S, Cl and Br. These types of deposits are formed by evaporation of salt-laden brine that precipitates sulfates, other salts and cemented sand grains. These results also suggest that liquid water existed in vast quantities on ancient Mars (McSween et al. 2011).

In December 2013, the Chang'e-3 spacecraft, carrying the Yutu rover, successfully landed in the northern part of Mare Imbrium on the Moon. The landing site of Chang'e-3 is located at (44.1260°N 19.5014°W), which is quite close to the boundary of two disparate geological units. Mare Imbrium has sequences of long basaltic lava flows that flooded the basin (Zhao et al. 2014). Based on the distribution of Ti on the Moon, basaltic lava that flowed around the landing area was high-Ti mare basalt. The boundary between high-Ti and low-Ti basalt was identified on false color images from Clementine, and this boundary is located to the northeast of Chang'e-3. We also observed many outcrops of bedrock on the rim of a crater that is 400 m in diameter and lies to the west of Chang'e-3 as identified in Pancam images. Geochemical investigations are an important part of characterizing a landing site, which includes chemistry, mineralogy and the texture of surface material. Data acquired by APXS can help us understand the chemical compositions and identify minerals in lunar soils and rocks. The analysis of lunar rocks near the landing site will be compared with the analysis of basalt samples from the Apollo program. The combined data set of measurements made by APXS

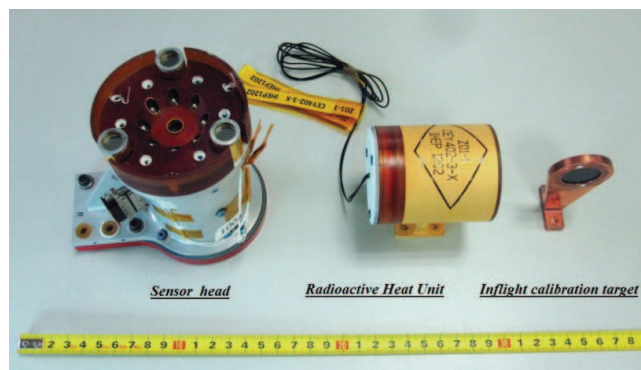


Fig. 1 APXS sensor head, RHU and calibration target.

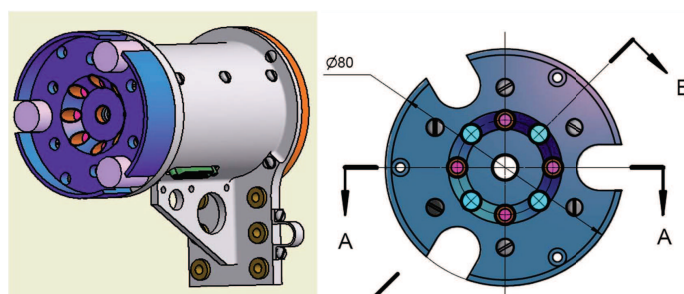


Fig. 2 APXS sensor head.

and Infrared spectra (Liu et al. 2014) can reveal the rock types and their mineral assemblage, and improve interpretation of Mare Imbrium magmatic evolution and geological history.

### 3 INSTRUMENT DESCRIPTION

APXS is mounted on a robotic arm attached to the Yutu rover, which on command brings the sensor head close to the lunar surface. The APXS instrument consists of a sensor head mounted on the arm, an in-flight calibration target, a radioactive heating unit (RHU) and main electronics (Fig. 1). The specifications of components in APXS are listed in Table 2. APXS involves the measurement of characteristic X-rays emitted from the sample due to the processes of PIXE and XRF. The radioactive sources ( $4 \times$ )  $^{55}\text{Fe}$  and ( $4 \times$ )  $^{109}\text{Cd}$  decay and produce alpha particles and X-rays. When alpha particles and X-rays interact with atoms in the surface material, they knock electrons out of their orbits, producing characteristic X-rays that can be measured with the silicon drift detector (SDD). The elements and their concentrations can be determined by analyzing their peak energies and intensities. The penetration depth of APXS radiation is only several micrometers into the surface of a sample.

The sensor head ( $\sim 752$  g, 1.2 W) is comprised of an SDD and eight excitation sources (Fig. 2). Use of the SDD with an active area of  $7 \text{ mm}^2$ , a  $2 \mu\text{m}$  thick Be window and an energy resolution of about 135 eV at 5.9 keV permits high-resolution measurement. Figure 3 shows the measurement geometry of the sensor head and a sample at a distance of 10 mm. A circular region on the Moon that emits characteristic X-rays that can be detected by SDD is called an effective detection area, which has a diameter of about 50 mm. The distance sensor is at the front of the APXS sensor head (light blue in Fig. 3). It can not only measure the distance between the head and target by the X-

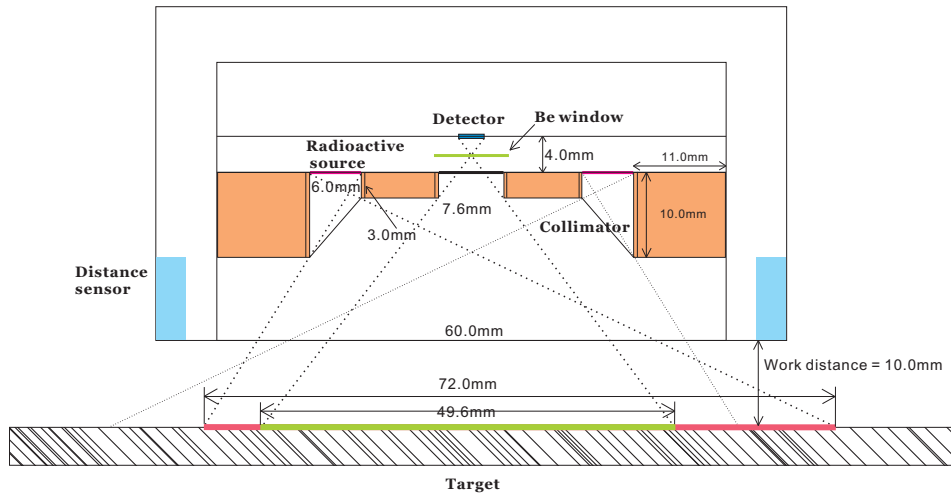


Fig. 3 Geometry of the APXS instrument (work distance 10 mm).

Table 2 APXS Specifications

Parameter	Value
<u>Sensor head</u>	
Detector type	Silicon Drift Detector
Energy range	0.39–22.1 keV
Energy resolution	135 eV@5.9 keV
Time resolution of data recording	Spectral, 8 s
Mass	752 g
Power	0.8 W
Radioactive source	4×70mCi <sup>55</sup> Fe+4×5mCi <sup>109</sup> Cd
Area	7 mm <sup>2</sup>
Width*length*height	80×115×124 mm <sup>3</sup>
<u>Radioactive Heating Unit</u>	
Mass	358 g
Power	4.25 W
Fuel	4.76 TBq <sup>238</sup> Pu
Width*length*height	70×58×85 mm <sup>3</sup>
<u>Calibration target</u>	
Material	Basalt
Mass	24 g
Target size	Φ23 mm, 3 mm in thickness

Table 3 Chemical Compositions of the APXS Calibration Target

Element	Concentration (wt%)	Element	Concentration (wt%)
Na	3.12	Fe	7.77
Mg	6.07	Mn	0.111
Al	7.13	P	0.222
Si	21.56	Cr	0.049
K	1.42	Ni	0.034
Ca	5.11	S	0.26
Ti	1.23		



**Fig. 4** View of the APXS calibration target.

**Table 4** Characteristics of the Radioactive Sources  $^{55}\text{Fe}$  and  $^{109}\text{Cd}$  used in the APXS Instrument

	Energy (keV)	Relative intensity
$^{55}\text{Fe}$ (Half-life: 2.744 yr)		
Mn $K_{\alpha}$	5.90	24.4%
Mn $K_{\beta}$	6.49	2.85%
$^{109}\text{Cd}$ (Half-life: 1.264 yr)		
XR $K_{\alpha 2}$	21.99	29.7%
XR $K_{\alpha 1}$	22.163	56%
XR $K_{\beta 3}$	24.912	4.79%
XR $K_{\beta 2}$	25.455	2.31%
$\gamma$	88	3.7%

ray counting rate, but also prevent the head from moving too close to the target which might cause mechanical damage.

The RHU is employed to provide a heat source ( $\sim 4\text{ W}$ ) that helps the sensor head survive a cold lunar night. RHU incorporates  $^{238}\text{Pu}$  with a strength 4.76 TBq as fuel. The RHU is mounted at the front of the rover. During a lunar night, the robotic arm would be raised and retracted so the position of the sensor head would be close to the RHU (Cui et al. 2014).

The APXS calibration target is a slab of well-characterized basaltic rock ( $\Phi 20\text{ mm} \times 5\text{ mm}$ ) fixed in an aluminum frame with a copper coating (thickness  $10\ \mu\text{m}$ ) (Peng et al. 2014). While the Yutu rover is working on the surface of the Moon, this target is used to periodically check the ongoing performance and calibration of the APXS instrument (Fig. 4). The basaltic sample in the target is from Liuhe District, Jiangsu Province, in east China. Major element concentrations are listed in Table 3.

The major sources in the instrument are a set of eight radioactive sources,  $4 \times ^{55}\text{Fe}$  and  $4 \times ^{109}\text{Cd}$ , that excite the target via primary X-rays at 5.90, 6.49, 22.16 and 24.94 keV (Table 4). Based on the theory of characteristic X-ray emission,  $^{55}\text{Fe}$  can excite the characteristic X-ray of  $Z = 11(\text{Na}) \sim 24(\text{Cr})$ . The lighter the atomic weight  $Z$  is, the weaker the X-ray fluorescence becomes. In principle,  $^{109}\text{Cd}$  can excite the characteristic X-ray of  $Z = 11(\text{Na}) \sim 42(\text{Mo})$ . Despite the ability to excite Mn, the energy of scattering off  $^{55}\text{Fe}$  from the source is overlapped with that from  $K_{\alpha}$  of Mn, which implies that its concentration in the sample cannot be determined. The lighter elements, Na, P and S, all have lower production cross-sections. These trace elements in lunar soils and rocks cannot be detected. In summary, using the sources  $^{55}\text{Fe}$  and  $^{109}\text{Cd}$ , APXS could detect major elements (Mg, Al, Si, K, Ca, Ti, Fe) and several trace elements (Ni, Sr, Y, Zr).

## 4 APXS DATA PROCESSING

APXS produces two data files for each measurement. The channel-count data are identified with “PIXS-E,” which could be used for analyzing the concentrations of elements. The data file records parameters describing the robotic arm, the temperatures of the APXS sensor head and main electronics and the 2148 channel counts each 8 s. The arm parameters are used to determine APXS operating modes and the temperature can help us correct for the effect of temperature. The other file, named “PIXS-C,” records the X-ray counting rate from the distance sensor, which can be used to calculate the work distance for analysis of a lunar sample.

### 4.1 Description of Operating Modes

APXS has three operating modes: calibration mode, distance sensing mode and in-situ detection mode. During the calibration mode, the robotic arm will retract and the APXS sensor head is aimed at the calibration target. In the “PIXS-E” data, the column representing operating mode is filled with the number “1.” When APXS approaches a lunar sample and attempts to analyze it, the distance sensor at the front of the sensor head will collect the counting rate to determine the work distance. This is called distance sensing mode, which is denoted with the number “2” in PIXS-E data. When the APXS sensor head arrives at the designated location and begins in-situ analysis, this is called in-situ detection mode and is denoted with the number “3.” All the others are denoted with “0” in PIXS-E data.

### 4.2 Work Distance Calculation

The work distances for the three different operating modes are calculated with different methods. For the calibration mode, the work distance  $d$  is 1.0 cm. For the distance sensing mode, the work distance  $d$  is 0. For the in-situ detection mode,  $d$  is calculated based on the counting rate data. The polynomial fitting equation is expressed as follows:

$$d = (P_0 + P_1 \cdot C + P_2 \cdot C^2 + P_3 \cdot C^3 + P_4 \cdot C^4),$$

where  $d$  is the work distance and  $P_i$  are the parameters in the given 4th order polynomial fitting equation. The values of these parameters are listed in Table 5.  $C$  is the counting rate collected when the sensor head is deployed to the designated location. In order to obtain the correct work distance, the selected value of  $C$  for calculating  $d$  is the average of eight counting rates in the first effective row of data. We compare all the counting rate data from top to bottom. The first row, in which all the eight values are less than 550, is defined as the first effective row of data.

**Table 5** Parameter Values for Work Distance Calculation used during in-situ Detection Mode

Parameter	2013-12-15	2014-01-01	2014-02-01	2014-03-01
$P_0$	233.291	239.165	241.244	243.23
$P_1$	-1.92169	-2.03867	-2.10878	-2.17487
$P_2$	0.00692733	0.00764009	0.00809416	0.00852927
$P_3$	-1.14E-05	-1.32E-05	-1.43E-05	-1.54E-05
$P_4$	6.92E-09	8.45E-09	9.39E-09	1.03E-08

Distance calibration experiments in a laboratory were performed in March 2013 before Chang'e-3 was launched. These experiments were carried out at room temperature in a vacuum container with residual pressure of less than 10 Pa. The sensor head of APXS was mounted on a movable platform, which could be used to control the distance between the head and sample with an error of  $\pm 0.01$  mm. Lunar simulants were used as samples in these experiments. The sensor head collected the counting

rate data at distances ranging from 3 mm to 60 mm at intervals of 3 mm or 5 mm. A curve could be obtained if the distance is plotted on the X axis and the counting rate on the Y axis. We fit the curve with the 4th order polynomial equation and calculated the parameters  $P_i$ . However, these parameters will change along with the radioactivity of excitation sources because of their decay. The parameter values for different dates are listed in Table 5.

#### 4.3 Correction for the Effect of Temperature

A traditional but effective calibration includes a gain ( $k$ , in keV Channel<sup>-1</sup>) that varies as a function of temperature and an offset ( $b$ ) yielding the relationship (VanBommel 2013):  $E = C \cdot k + b$ , where  $E$  is the X-ray energy in keV and  $C$  is the channel number.

We can pick several well-known peaks in the spectrum and derive the relationship between peak center and characteristic X-ray energy on an element.  $k$  and  $b$  can be calculated with the least squares method.

In this study, we chose nine peaks on the APXS spectrum, including Si K<sub>α</sub> (1.74 keV), K K<sub>α</sub> (3.31 keV), Ca K<sub>α</sub> (3.69 keV), Ti K<sub>α</sub> (4.51 keV), Ti K<sub>β</sub> (4.93 keV), Fe K<sub>β</sub> (7.06 keV), Ni K<sub>α</sub> (7.74 keV) and Cu K<sub>α</sub> (8.04 keV). All these peaks are clearly identified and have narrow FWHMs. We built the linear relationship between the channel and peak energy and calculated the values of slope and intercept for each measurement.

#### 4.4 Dead Time Correction

The fourth step is dead time correction. A detector that sequentially responds to individual events requires a minimum amount of time that should separate two events in order that the events be recorded as two separate events. This minimum time is called the “dead time.” The dead time  $t$  of APXS is 12.5 μs. The value was set in the main electronics component during development of the instrument. Dead time correction could be calculated with the following expression

$$\text{APXS}_2 = \frac{\text{APXS}_1}{8 - t \cdot \text{APXS}_1},$$

where APXS\_1 is the number of counts from each channel before dead time correction is applied, APXS\_2 is the counts after correction and  $t$  is the dead time of APXS.

### 5 OBTAINED DATA

APXS has carried out two calibrations and two lunar soil detections. Figure 5 shows a map of the transverse path for the Yutu rover on the Moon and locations where APXS measurements were acquired. On 2013 December 22, the Yutu rover arrived at a point south of the lander (which corresponds to point N0106) and APXS was powered on for the first time. At this location, APXS performed the first calibration after landing on the Moon. During seven minutes, APXS obtained 93 frames of scientific data. On 2013 December 24, APXS analyzed the first lunar soil sample and recorded 1100 frames of scientific data for two and a half hours. After the first night on the Moon, the Yutu rover successfully woke up on 2014 January 12. The second calibration lasted about 35 minutes and 304 frames of data were obtained. On 2014 January 14, APXS performed the second lunar soil analysis for about one hour and 584 frames of scientific data records were acquired.

### 6 INITIAL RESULTS FROM APXS

In the present study, we analyzed data from the first calibration and lunar soil survey. Corrections for the effect of temperature and dead time were performed using the method presented above. Based on



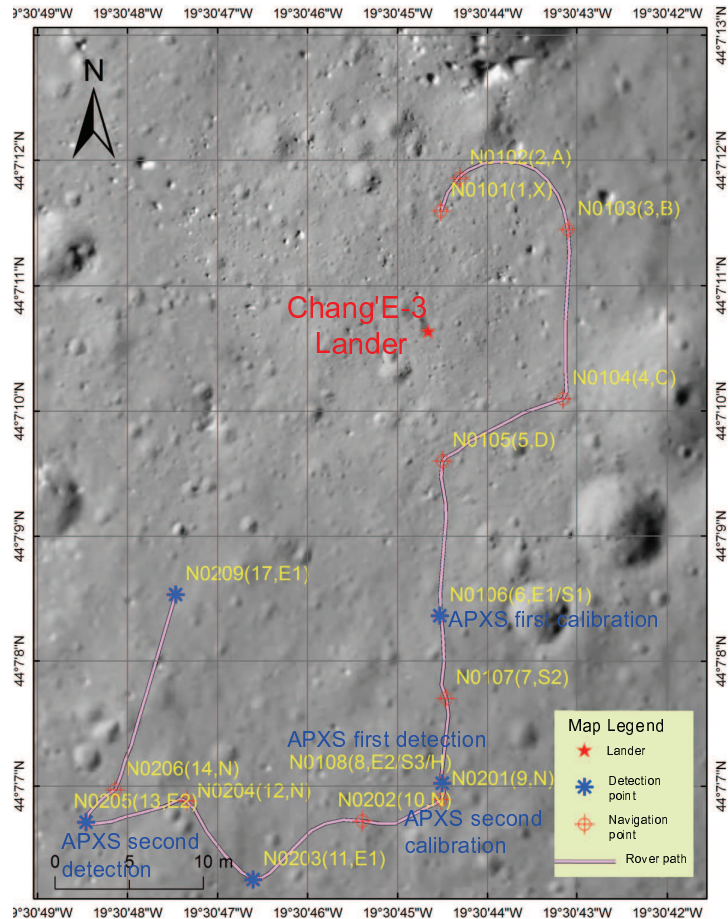


**Fig. 5** Map of the path that the Yutu rover traversed on the Moon and the locations where APXS was operated.

the spectra, we identified major element peaks and compared semi-quantitative results of elemental abundance in the calibration basalt and lunar soil.

Figure 6 shows APXS results of the calibration target and lunar soil. Major elements Mg, Al, Si, K, Ca, Ti and Fe are identified. In this study, we build a linear relationship between elemental peaks and energies in order to convert spectral channel to energy. The elemental peaks and their energies are listed in Table 6. For the calibration target, the slope and intercept of the regression line are  $0.0109 \pm (1.43 \times 10^{-4})$  and  $0.562 \pm 0.072$  respectively, and the correlation coefficient is 99.86%. For lunar soil, the slope and intercept are  $0.0109 \pm (1.38 \times 10^{-4})$  and  $0.501 \pm 0.070$  respectively, and the correlation coefficient is 99.87%. To compare the two spectra, integration time has been normalized, as shown in Figure 7. The energy resolution of APXS is estimated to be 138 eV at 5.9 keV, which is good enough to resolve the K-lines of elements ( $Z = 12 \sim 41$ ).

In this study, the spectral background is fitted with a third order polynomial curve. The peaks are fitted with the Peakfit program. The peak areas and their ratios with Si are listed in Table 7. For

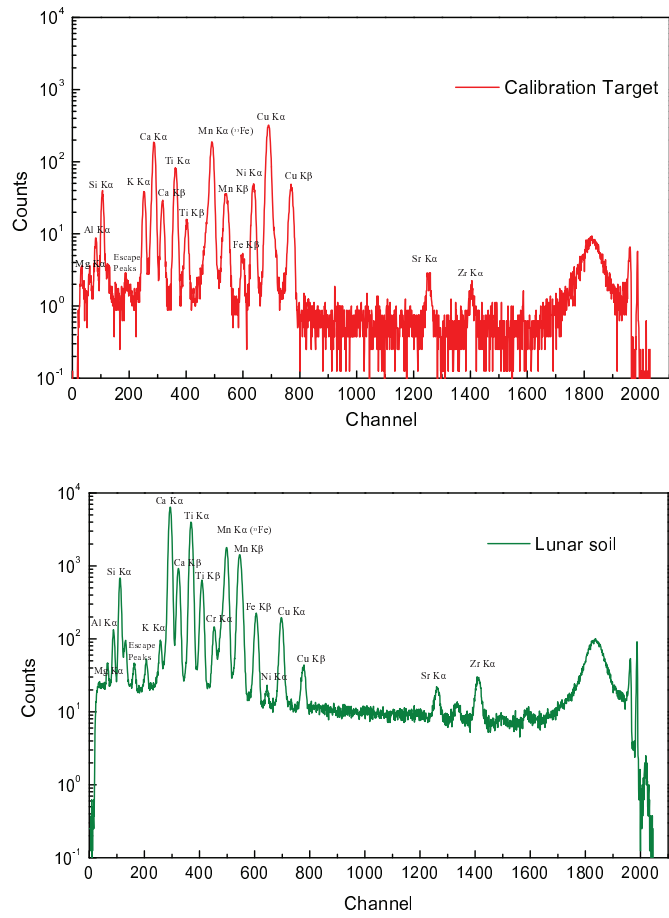


Fig. 6 Spectra of channel count data acquired by APXS of the calibration target and lunar soil.

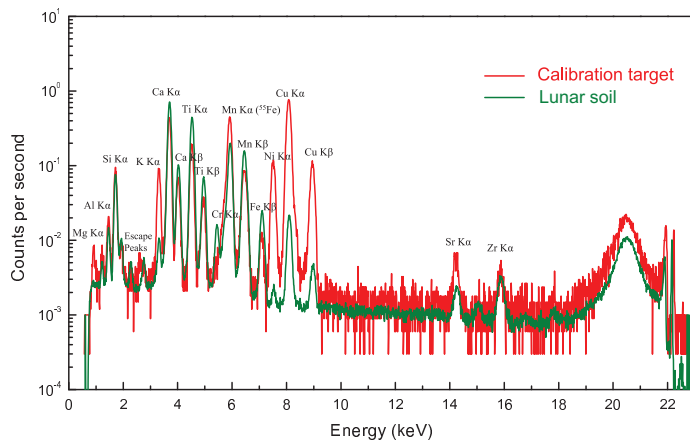


Fig. 7 APXS spectra of the calibration target and lunar soil.

**Table 6** Elemental Peaks and Energies Chosen for Linear Fitting

Peak	Calibration	Lunar soil	Energy (keV)
Si K <sub>α</sub>	106	112	1.74
K K <sub>α</sub>	252	258	3.31
Ca K <sub>α</sub>	287	294	3.69
Ti K <sub>α</sub>	364	370	4.51
Ti K <sub>β</sub>	403	409	4.93
Fe K <sub>β</sub>	597	606	7.06
Ni K <sub>α</sub>	637	645	7.74
Cu K <sub>α</sub>	690	697	8.04
Cu K <sub>β</sub>	770	777	8.907

**Table 7** Elemental Peak Areas and Ratios between the Calibration Target and Lunar Soil

	First calibration			First lunar soil detection		
	Peak area (counts)	Relative error of peak area (counts)	Peak area ratio	Peak area (counts)	Relative error of peak area (counts)	Peak area ratio
Mg K <sub>α</sub>	149.09	22.65	0.05	429.98	17.86	0.03
Al K <sub>α</sub>	587.46	37.66	0.21	2220.63	43.02	0.17
Si K <sub>α</sub>	2832.71	77	1	13321	113.4	1
K K <sub>α</sub>	3367.83	83.35	1.19	1999.38	41.37	0.15
Ca K <sub>α</sub>	16728.6	184.61	5.91	153755	358.77	11.54
Ti K <sub>α</sub>	7823.04	126.18	2.76	103376	294.38	7.76
Fe K <sub>α</sub>	2789.41	90	0.98	34114.3	292.51	2.56

all the seven elements, we compared their peak areas near the K<sub>α</sub> line. Note that lunar soil is more enriched in Mg and Al than the calibration basalt, and also has higher amounts of Ca, Ti and Fe. However, K in lunar soil is significantly less than the calibration basalt.

In this study, we only compared the ratios of elements in calibration basalt and lunar soil. The absolute concentrations of these elements have not yet been obtained, because the calibration spectrum measured by APXS on the Moon is not only produced by the calibration basalt. It has been noticed that the area of the APXS sensor head exceeds the effective area of the basalt during calibration. This means that in the calibration mode, APXS not only detected characteristic X-rays emitted from the basalt but also the Al holder with Cu coating. This is the reason why there are strong Cu peaks in the calibration spectrum. In the future, we will perform calibration experiments to eliminate the X-ray contribution of the holder, and calculate the absolute elemental concentrations of two lunar soils based on two sets of in-situ detection data.

## 7 CONCLUSIONS

APXS is an important payload mounted on the Yutu rover, part of the Chang'e-3 mission, with the goal of determining the chemical composition of a sample of lunar soil and rocks. APXS has analyzed the calibration target and lunar soil once for the first lunar day and again for the second lunar day. The total detection time lasted about 266 min and more than 2000 frames of data were acquired. APXS has three operating modes: calibration mode, distance sensing mode and detection mode. In the detection mode, work distance was calculated from the X-ray counting rate collected by SDD. Correction for the effect of temperature has been performed to convert the channel number of each spectrum to X-ray energy. Dead time correction tries to eliminate the systematic error in quantifying the activity of an X-ray pulse in a sample and derive the real count rate. Here, we report

data obtained from APXS and initial results during the first and second lunar days for the Yutu rover. In this study, we analyze data from the calibration target and lunar soil on the first lunar day. Seven major elements, including Mg, Al, Si, K, Ca, Ti and Fe, have been identified. Comparing the peak areas and ratios of calibration basalt and lunar soil, the landing site was found to be depleted in K, and have lower Mg and Al but higher Ca, Ti and Fe. In the future, we will obtain elemental concentrations of lunar soil near the Chang'e-3 landing site using APXS data.

**Acknowledgements** This work was funded by the National Natural Science Foundation of China (Grant Nos. 41303051 and 41490633), and Macau FDCT program (Grant No. 020/2014/A1).

## References

- Campbell, J. L., Lee, M., Jones, B. N., et al. 2009, *Journal of Geophysical Research (Planets)*, 114, 4006
- Campbell, J. L., Andrushenko, S. M., Taylor, S. M., & Maxwell, J. A. 2010, *Journal of Geophysical Research (Planets)*, 115, 4009
- Campbell, J. L., Perrett, G. M., Gellert, R., et al. 2012, *Space Sci. Rev.*, 170, 319
- Cui, X. Z., Wang, H. Y., Peng, W. X., et al. 2014, in *Lunar and Planetary Inst. Technical Report*, 45, Lunar and Planetary Science Conference, 1373
- Economou, T. 2001, *Radiation Physics and Chemistry*, 61, 191
- Foley, C. N., Economou, T. E., Clayton, R. N., & Dietrich, W. 2003, *Journal of Geophysical Research (Planets)*, 108, 8095
- Gellert, R., Campbell, J. L., King, P. L., et al. 2009, in *Lunar and Planetary Inst. Technical Report*, 40, Lunar and Planetary Science Conference, 2364
- Gellert, R., Rieder, R., Brückner, J., et al. 2006, *Journal of Geophysical Research (Planets)*, 111, E02S05
- Ip, W.-H., Yan, J., Li, C.-L., & Ouyang, Z.-Y., 2014, *RAA (Research in Astronomy and Astrophysics)*, 14, 1511
- Klingelhöfer, G., Brückner, J., D'Uston, C., Gellert, R., & Rieder, R. 2007, *Space Sci. Rev.*, 128, 383
- Liu, B., Li, C.-L., Zhang, G.-L., et al. 2014, *RAA (Research in Astronomy and Astrophysics)*, 14, 1578
- Maxwell, J., Teesdale, W., & Campbell, J. 1995, *Nuclear Instruments and Methods in Physics Research Section B: Beam Interactions with Materials and Atoms*, 95, 407
- McSween, H. Y., McNutt, R. L., & Prettyman, T. H. 2011, *Proceedings of the National Academy of Science*, 108, 19177
- Peng, W. X., Wang, H. Y., Cui, X. Z., et al. 2014, in *Lunar and Planetary Inst. Technical Report*, 45, Lunar and Planetary Science Conference, 1699
- Pullan, D., Sims, M. R., Wright, I. P., Pillinger, C. T., & Trautner, R. 2004, in *ESA Special Publication*, 1240, *Mars Express: The Scientific Payload*, ed. A. Wilson & A. Chicarro, 165
- Rieder, R., Economou, T., Wanke, H., et al. 1997, *Science*, 278, 1771
- Rieder, R., Gellert, R., Brückner, J., et al. 2003, *Journal of Geophysical Research (Planets)*, 108, 8066
- Schmanke, D., Klingelhöfer, G., Girones Lopez, J., Brückner, J., & D'Uston, C. 2010, in *European Planetary Science Congress 2010*, 898
- Shanmugam, M., Murty, S., Acharya, Y., et al. 2014, *Advances in Space Research*, 54, 1974
- VanBommel, S. 2013, *Analysis and Calibration of the MER-A APXS Alpha Particle Backscatter Spectra*, PhD Thesis, Department of Physics, University of Guelph
- Zhao, J., Huang, J., Qiao, L., et al. 2014, *Science China Physics, Mechanics, and Astronomy*, 57, 569